coasts

MDPI

Article

From Coastal Flooding to Residual Beach Functionality: Implications of Sea-Level Rise for Coastal Management in Southern Spain

Antonio Contreras-de-Villar [1], Francisco Contreras-de-Villar [1], Juan M. Vidal-Perez [2], Cristina Perez-Moreno [1], Jose J. Alonso del Rosario [2], Patricia Lopez-Garcia [1], Bismarck Jigena-Antelo [1] and Juan J. Muñoz-Perez [1,*]

[1] Coastal Engineering Research Group, University of Cadiz, 11510 Puerto Real, Spain; antonio.contreras@uca.es (A.C.-d.-V.); francisco.contreras@uca.es (F.C.-d.-V.); cristina.perezmoreno@uca.es (C.P.-M.); patricia.lopezgarcia@uca.es (P.L.-G.); bismarck.jigena@uca.es (B.J.-A.)
[2] Centro Andaluz Superior de Estudios Marinos (CASEM)—Escuela de Ingenieria Naval y Oceanica, University of Cadiz, 11510 Puerto Real, Spain; juan.vidal@uca.es (J.M.V.-P.); josejuan.alonso@uca.es (J.J.A.d.R.)
* Correspondence: juanjose.munoz@uca.es

Abstract

Sea-level rise may substantially reduce the dry space available on sandy beaches, although its effects depend strongly on local beach characteristics. This study evaluates the residual spatial functionality of five beaches in southern Spain using two normalized indicators: residual available surface area (F_A) and residual available beach width (F_W). Both express the proportion of dry beach space remaining relative to a common present-day reference condition without wave run-up. The analysis builds on previously calculated inundation results for present conditions and Representative Concentration Pathway (RCP) 4.5 and RCP 8.5 scenarios for 2026–2045 and 2081–2100, including astronomical tide, meteorological residual, sea-level rise, and wave run-up. Marked differences are observed among the studied beaches across both time periods. Under RCP 4.5 in 2026–2045, Torreguadiaro retains 85.1% of its reference area and 79.8% of its reference mean width. Rinconcillo retains 31.9% and 38.7%, respectively. Under RCP 8.5 in 2081–2100, these values decrease to 75.6% and 65.3% at Torreguadiaro. At Rinconcillo, they decrease to 7.1% and 17.6%. F_A and F_W also evolve differently among sites: their values remain relatively close at Malagueta but diverge markedly at Rinconcillo under the most severe scenario. Joint consideration of F_A and F_W therefore provides complementary information on the amount and configuration of residual dry beach space and may support comparison among beaches from a coastal management perspective.

Keywords: sea-level rise; beach functionality; coastal flooding; beach width; coastal management

Check for updates

Academic Editor: Athanassios A. Dimas

Received: 16 August 2026
Revised: 7 October 2026
Accepted: 10 October 2026
Published: 16 October 2026

Copyright: © 2026 by the authors. Licensee MDPI, Basel, Switzerland. This article is an open access article distributed under the terms and conditions of the Creative Commons Attribution (CC BY) license.

1. Introduction

Sea-level rise is one of the major challenges facing coastal management in the coming decades. Its effects may intensify coastal flooding and erosion, reduce available space, and increase the exposure of ecosystems and infrastructure. These impacts are part of broader climate-related changes affecting both natural and socioeconomic systems [1–5]. In particular, observed sea-level rise and its potential future acceleration are relevant drivers of coastal evolution [6–8].

Beaches simultaneously provide environmental, recreational, and coastal protection functions. Their vulnerability should therefore not be assessed solely through shoreline

displacement or inundated area. Progressive reductions in beach width and dry surface area may compromise wave-energy dissipation and recreational use. They may also leave less space for future coastal adaptation [9].

Studies in the Gulf of Cadiz have already shown the sensitivity of these systems to sea-level rise and its potential effects on coastal erosion [10]. Coastal vulnerability has consequently been assessed using indices, inundation mapping, statistical analyses, and deterministic models of varying complexity [11–15].

The loss of beach surface area and width can simultaneously affect coastal protection, recreational use, and socioeconomic value [16–18]. Studies conducted under different coastal settings have also reported highly variable responses to sea-level rise, coastal flooding and shoreline change [19–24].

Beach response also depends on morphological and sedimentary characteristics. Beach slope, sediment size, profile geometry, and sediment availability influence coastal behavior. These aspects have been studied along the Cadiz coast using beach-profile analysis, geological controls, topographic monitoring, and sediment characterization [25–29]. RPAS techniques have further expanded the possibilities for monitoring beaches and dunes [28]. Beach nourishment is another relevant measure for maintaining or restoring beach space. Its performance depends on beach geometry and the characteristics of the sediment used [30–32].

In this context, assessing coastal resilience requires linking physical processes with indicators directly related to beach functionality. Inundation maps identify potentially affected areas but do not necessarily express the functional consequences of reduced available space. Two beaches exposed to similar sea-level rise may retain very different amounts of dry surface area and width. This response depends strongly on their local geomorphology. Traditional inundation indicators can therefore be complemented by parameters describing the residual capacity of the beach.

This issue is particularly relevant along the southern Spanish coast. The Atlantic and Mediterranean sectors differ markedly in tidal regime, wave climate, beach slope, and sedimentary characteristics. Previous studies in the area have examined morphological evolution, sediment transport, and responses to coastal interventions [27,33]. These contrasting conditions provide a suitable setting for comparison. The same climatic forcing may produce very different functional consequences among beaches. Specific assessments and official maps of coastal vulnerability and flooding are also available for the region [34].

A recent study examined five representative beaches in Cadiz and Malaga using a physically based approach [35]. The analysis combined sea-level rise, astronomical tide, meteorological residuals, and wave run-up. That analysis quantified inundation and the resulting losses of dry beach surface area and width under present and future scenarios. It also showed the importance of wave run-up and the contrasting responses of Atlantic and Mediterranean beaches.

Those loss-based metrics characterize the magnitude of beach-space reduction, but they do not explicitly describe the proportion of the original dry beach that remains available under each scenario. This distinction is relevant for coastal management. Adaptation decisions depend not only on how much beach space is lost, but also on how much remains. It is also useful to determine whether residual surface area and width evolve in parallel. Joint consideration of these two spatial dimensions may therefore provide additional information on the configuration of the remaining dry beach.

Accordingly, this study evaluates the residual spatial functionality of the same five sandy beaches. Two normalized indicators are used: residual available surface area (F_A) and residual available beach width (F_W). Rather than constituting a new hydrodynamic assessment, the analysis builds on previously calculated inundation results and reinterprets them in terms of remaining beach space. Particular attention is given to the joint response

of F_A and F_W and to whether the two dimensions evolve similarly among beaches and scenarios. The implications of these residual patterns for coastal management and adaptation are subsequently discussed.

2. Materials and Methods

2.1. Study Area and Input Data

The analysis considers five sandy beaches located along the coasts of Cadiz and Malaga in southern Spain: Los Toruños, Hierbabuena, Rinconcillo, Torreguadiaro, and Malagueta. These sites represent contrasting conditions between mesotidal Atlantic sectors and microtidal Mediterranean sectors and also differ appreciably in beach width, slope, sediment size, and backshore configuration. Their geographical distribution and local coastal settings are shown in Figure 1.

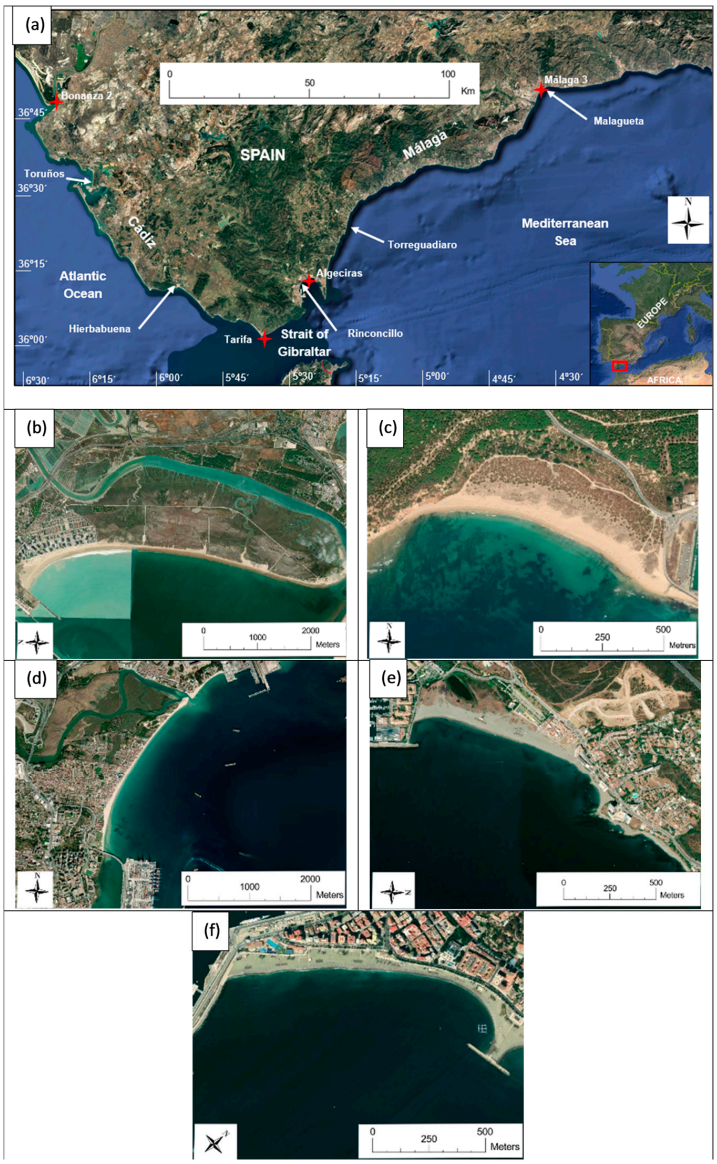

Figure 1. Location and coastal setting of the five study beaches in southern Spain. (**a**) Geographical location of the study sites along the Atlantic and Mediterranean coasts; (**b**) Los Toruños; (**c**) Hierbabuena; (**d**) Rinconcillo; (**e**) Torreguadiaro; and (**f**) Malagueta. Panels (**b**–**f**) show aerial views of each beach and its immediate surroundings. White arrows indicate the five study beaches, while the four red stars identify geographical reference locations (Bonanza, Algeciras, Tarifa, and Málaga). The red rectangle in the European inset map identifies the study area. Source: Google Earth.

The selected beaches and the topographic and bathymetric datasets have been described previously [35]. That study extended the analysis to all five beaches and provided comparable estimates of inundation, dry beach area, and available width.

Emergent beach topography was derived from official coastal cartography supported by differential GPS surveys. The reported horizontal and vertical accuracies were 5 mm + 1 ppm and 10 mm + 1 ppm, respectively. Bathymetric data were obtained from the official coastal ecocartography and processed onto a 5 × 5 m grid. Cross-shore profiles were extracted at approximately 200 m intervals across the emerged and submerged beach. A total of 38 profiles were analysed. These comprised 7 at Los Toruños, 6 at Hierbabuena, 13 at Rinconcillo, 6 at Torreguadiaro, and 6 at Malagueta. All elevations used in the inundation analysis were referenced to the Lowest Low Water Level (LLWL).

The scenarios considered correspond to the periods 2026–2045 and 2081–2100 under RCP 4.5 and RCP 8.5. Regionalized projections and oceanographic data were obtained from official Spanish coastal sources. These included C3E, AEMET, Puertos del Estado, and coastal ecocartography datasets [36–42]. These calculations are not repeated here. Instead, the previously derived results are used as input data to assess the proportion of dry beach space remaining available under each scenario.

Long-term sea-level records additionally provide regional evidence of ongoing changes in relative sea level [43].

2.2. Inundation Scenarios

The inundation levels used in this study were obtained from Contreras-de-Villar et al. [35]. That analysis combined mean sea level, astronomical tide, meteorological residual, and wave run-up. Wave run-up was simulated using the IH2VOF model, whose development and application to wave transformation and uprush processes have been described previously [44,45]. Empirical formulations for wave setup, swash, and run-up also provide a well-established reference for this type of analysis [46].

Present-day conditions and four future scenarios were considered: RCP 4.5 and RCP 8.5 for 2026–2045 and 2081–2100. RCP 8.5 is retained as a high-end scenario and for consistency with the underlying inundation analysis [35]. It is not interpreted here as the expected future emissions pathway. For each case, the corresponding inundation level was intersected with the beach profiles. This procedure identified the inundated and remaining dry portions of the beach. The resulting calculations provided the dry beach surface area and mean dry beach width remaining under each scenario. These quantities had been previously obtained by Contreras-de-Villar et al. [35] and are used here as the input dataset for the residual-functionality analysis. No additional hydrodynamic simulations were performed in the present study. Accordingly, no additional field instruments or hydrodynamic modelling software were used in the present analysis. Details of the original datasets and modelling procedures are provided in [35].

2.3. Residual Functionality Indicators

Residual beach functionality was expressed as the proportion of dry beach surface area and dry beach width remaining available relative to the present-day reference condition. Two dimensionless indicators were defined:

$$F_A = \frac{A_s}{A_0} \cdot 100 \quad (1)$$

$$F_W = \frac{W_s}{W_0} \cdot 100 \quad (2)$$

where F_A and F_W are the residual available surface area and residual available beach width, respectively, expressed as percentages. A_S and W_S denote the dry beach surface area and mean dry beach width remaining under each considered scenario after including wave run-up. A_0 and W_0 denote the corresponding present-day reference surface area and width calculated without wave run-up. The same reference condition is used for all scenarios.

Consequently, present-day F_A and F_W values do not necessarily equal 100%. Their numerators correspond to present-day conditions including wave run-up, whereas A_0 and W_0 describe the present-day dry-beach geometry without wave run-up. For the future scenarios, the same A_0 and W_0 values are retained as denominators. This common baseline allows direct comparison among scenarios. It includes the reduction caused by present-day wave run-up and the additional reduction associated with future sea-level rise.

Both indicators range from 0 to 100%. Values close to 100% indicate that most of the reference dry beach space remains available, whereas values approaching zero indicate an almost complete loss of available dry beach space. No universal functionality thresholds are imposed because minimum requirements for beach area and width depend on beach use, morphology, and local management context.

To compare the relative behaviour of the two residual dimensions, the area–width differential was calculated as $D = F_A - F_W$. A value of $D = 0$ indicates equal proportional reductions in residual area and mean width. For example, $F_A = 70\%$ and $F_W = 70\%$ give $D = 0$ percentage points. Negative values indicate a proportionally greater reduction in residual area. Positive values indicate a proportionally greater reduction in residual mean width. When both F_A and F_W are zero, D is not interpreted because no residual beach dimension remains for comparison.

3. Results

Evolution of Residual Beach Functionality

The F_A and F_W values show a progressive reduction in available dry beach surface area and width as sea level increases. However, the magnitude of this reduction differs considerably among the five beaches. Differences are already apparent under present-day conditions when wave run-up is included and become more pronounced toward the end of the century. In addition, F_A and F_W do not evolve in parallel at all sites, indicating that residual surface area and residual beach width provide complementary information. The values obtained for each beach and scenario are summarized in Table 1.

Table 1. Residual beach functionality considering the effect of wave run-up.

Beach	Indicator	Present Day	2026–2045 RCP 4.5	2026–2045 RCP 8.5	2081–2100 RCP 4.5	2081–2100 RCP 8.5
Toruños	F_A (%)	0.0	0.0	0.0	0.0	0.0
	F_W (%)	0.0	0.0	0.0	0.0	0.0
Hierbabuena	F_A (%)	74.9	69.8	68.8	64.3	60.4
	F_W (%)	63.7	60.4	59.6	57.0	53.8
Rinconcillo	F_A (%)	40.2	31.9	29.4	17.7	7.1
	F_W (%)	47.3	38.7	34.4	23.2	17.6
Torreguadiaro	F_A (%)	89.2	85.1	82.0	79.7	75.6
	F_W (%)	84.4	79.8	77.0	72.4	65.3
Malagueta	F_A (%)	62.5	56.4	52.6	49.3	44.1
	F_W (%)	65.8	58.1	54.2	51.2	46.0

Note: F_A: residual available surface area; F_W: residual available beach width. Values are calculated relative to present-day reference condition without wave run-up. Source data were obtained from Contreras-de-Villar et al. [35].

Los Toruños represents the limiting case, with F_A and F_W equal to 0% under all scenarios considered. These zero values do not indicate the absence of a beach under the reference condition. Both A_0 and W_0 are non-zero. Under the present-day forcing, however, A_S and W_S become zero. Consequently, Equations (1) and (2) give $F_A = F_W = 0$.

Conversely, Torreguadiaro consistently retains the highest residual functionality. Under the end-of-century RCP 8.5 scenario, 75.6% of its reference surface area remains available. The corresponding residual mean width is 65.3%.

Hierbabuena shows an intermediate response. Its residual surface area decreases from 74.9% under present-day conditions to 60.4% under the end-of-century RCP 8.5 scenario. Over the same range of conditions, residual mean beach width decreases from 63.7% to 53.8%.

Rinconcillo exhibits a particularly pronounced reduction. Its residual surface area decreases from 40.2% under present-day conditions to only 7.1% under the end-of-century RCP 8.5 scenario. Residual beach width also decreases substantially, from 47.3% to 17.6% over the same range of conditions. Under the end-of-century RCP 8.5 scenario, the area–width differential reaches $D = -10.5$ percentage points. Residual width therefore remains proportionally larger than residual surface area.

Malagueta shows a more gradual reduction. Under the end-of-century RCP 8.5 scenario, approximately 44.1% of its reference surface area and 46.0% of its reference mean width remain available. In contrast to Rinconcillo, F_A and F_W remain relatively close throughout the considered scenarios. Overall, similar sea-level-rise scenarios produce markedly different residual responses among beaches. Differences occur both in the amount of dry space remaining and in the relative evolution of surface area and width.

4. Discussion

4.1. Differences Among Beaches

The differences observed among the studied beaches cannot be attributed solely to the magnitude of sea-level rise. Beach-profile geometry controls how a vertical increase in water level translates into a horizontal loss of dry beach space. Gently sloping and low-lying profiles are generally associated with greater inland penetration of inundation.

This behavior is particularly evident at Los Toruños and Rinconcillo, where mean beach slopes are approximately 2.0% and 3.0%, respectively. By contrast, Torreguadiaro and Malagueta have slopes exceeding 6% and retain a larger proportion of their reference dry beach space [35]. Nevertheless, beach slope alone does not account for all the differences observed.

Hierbabuena illustrates this point. With an intermediate mean slope of approximately 5.5%, it retains a substantial proportion of both its reference surface area and width. Beach-profile configuration, tidal regime, and wave conditions also influence the local response. These effects were examined in the underlying inundation analysis [35]. Residual functionality therefore reflects both the imposed water levels and the local beach configuration. It should not be interpreted as a response to sea-level-rise magnitude alone.

Comparison of F_A and F_W provides complementary information because the two indicators describe different spatial dimensions of the remaining dry beach. F_A expresses the proportion of total dry surface area retained, whereas F_W represents the proportion of residual mean beach width. If the reduction in dry beach space were geometrically proportional, both indicators would be expected to evolve similarly. This is approximately the case at Malagueta, where F_A and F_W remain close under the end-of-century RCP 8.5 scenario (44.1% and 46.0%, respectively). In contrast, Rinconcillo retains only 7.1% of its reference dry surface area but 17.6% of its reference mean width under the same scenario. Considering F_A and F_W together shows whether residual surface area and mean width evolve in a similar way. This information is not provided by either indicator alone.

These site-specific differences raise the question of whether the observed range of residual responses is consistent with spatial changes reported for other sandy coastal settings. This broader context is examined in the following section.

4.2. Residual Beach Space in the Context of Other Coastal Settings

The spatial responses obtained for the five beaches fall within the broad variability reported for sandy coasts elsewhere (Table 2). Direct numerical comparison nevertheless requires caution. Published studies differ in forcing, morphological setting, reference conditions, and response metrics. For this reason, the values in Table 2 are retained in their original form rather than converted into F_A or F_W.

Table 2. Quantitative comparison of morphological settings and reported spatial responses to sea-level rise in selected sandy coastal environments.

Study and Region	Coastal Setting	Mean Tidal Range (Approx., m)	Morphological Context	SLR or Forcing	Reported Spatial Response
Brunel and Sabatier [47], Provence, France	Pocket beaches	0.3	Beach Width 5–47 m; slope 1–3.6%; landward constrained	+0.44 m by 2100	Beach-surface loss: 75–97%
Bon de Sousa et al. [48], southern Portugal	Platform beaches	2.2	32 beaches; 94 profiles; cliff-backed	+0.5/+1.0 m	Mean beach-width reduction: 5.8/9.6 m
Thieblemont et al. [49], Aquitaine, France	Open sandy coast	3.2–3.7	Low-gradient nearshore; spatially variable profile slopes	SLR to 2100	Shoreline retreat: ~58–200 m
Castelle et al. [50], SW France	Open beach–dune coast	3.2–3.7	269-km high-energy sandy coast	Observed, 1984–2020	Mean shoreline trend −0.55 m yr^{-1}
Masselink et al. [51], SW England	Embayed beach–dune systems	~4–6 m	25 dune-backed systems	SLR to 2100	Dune-foot retreat: ~0.5 m yr^{-1}; ~20–75 m by 2100
Present study, Atlantic Spain	Open sandy beaches	0.6–2.4	Mean beach slope: ~2.0–5.5%	RCP4.5 and RCP8.5	RCP8.5 (2100): F_A = 0–60.4%; F_W = 0–53.8%
Present study, Mediterranean Spain	Open and locally constrained sandy beaches	<0.6	Mean beach slope: ~3.0 to >6%	RCP4.5 and RCP8.5	RCP8.5 (2100): F_A = 7.1–75.6%; F_W = 17.6–65.3%

Note: Response metrics are reported according to the definitions used in the original studies. Beach-area loss, shoreline retreat, dune-foot retreat, and residual beach area or width are not directly equivalent. The values therefore provide quantitative context rather than a common response metric. Mean tidal ranges are approximate and may vary spatially within regional-scale studies.

Constrained beaches provide a relevant comparison. Brunel and Sabatier [47] projected losses of 75–97% of present beach surface for microtidal pocket beaches in Provence. Bon de Sousa et al. [48] projected mean beach-width reductions of 5.8 and 9.6 m for sea-level rises of 0.5 and 1.0 m, respectively. These studies show substantial spatial losses in beaches where landward adjustment is constrained by cliffs or other morphological boundaries (Table 2).

The studies in Table 2 do not indicate a simple relationship between tidal range and spatial beach response. Lower-gradient profiles can translate vertical water-level changes into larger horizontal displacements. However, local morphology and landward accommodation can substantially modify this response. The marked alongshore variability reported by Castelle et al. [50] within the same tidal setting further illustrates this point.

The present results show comparable variability within the Mediterranean sector. Under end-century RCP8.5 conditions, Torreguadiaro retains 75.6% of its reference area and 65.3% of its reference mean width. Rinconcillo retains only 7.1% and 17.6%, respectively. Despite their similar microtidal setting, the two beaches therefore show markedly different residual responses. Local beach morphology and configuration are thus important in modulating the spatial response to the imposed water levels.

The relationship between F_A and F_W provides an additional perspective on this variability. At Malagueta, their end-century values remain similar (F_A = 44.1%; F_W = 46.0%). At Rinconcillo, F_A decreases to 7.1%, whereas F_W remains at 17.6%. Mean width alone may therefore underrepresent spatial losses where dry-beach contraction varies alongshore.

Joint interpretation of F_A and F_W better describes the amount and configuration of the residual dry-beach space.

4.3. Implications for Coastal Management

Residual beach functionality complements inundation maps by describing the dry beach space remaining under each scenario. Inundation extent identifies the area reached by water but does not quantify the beach space that remains available. F_A and F_W address this distinction through residual surface area and mean width, respectively. Their joint interpretation can therefore support comparison of spatial consequences among beaches with different initial dimensions.

Residual beach width represents, in simple terms, the cross-shore space remaining between the sea and landward features. Its reduction may increase the exposure of dunes, promenades, infrastructure, and other coastal assets. Residual dry surface area provides a broader measure of the space that remains available. This space may support recreational and other beach-related uses. These two dimensions are therefore complementary from a management perspective: F_W describes the remaining cross-shore buffer, whereas F_A reflects the overall dry area retained. The usefulness of linking extreme water levels with consequences for coastal assets has also been demonstrated for critical infrastructure in southern Spain, where extreme-value analysis and topographic modelling have been combined to identify potentially inundated areas and support resilience measures [52].

The contrasting responses obtained here suggest that adaptation strategies should not be defined solely according to the climate scenario considered. Local beach characteristics and the type of residual space that remains are equally relevant. For example, a beach may retain a moderate mean width even after losing much of its total dry surface area. Rinconcillo shows this behavior under the most severe scenario. Beach nourishment, dune restoration, and preservation of sedimentary space may help maintain dry surface area and width. Their effectiveness, however, will depend on local conditions.

Adaptation should also be considered within broader coastal risk-management frameworks [53–57]. In this context, maintaining sufficient space within the beach system may facilitate both process-based solutions and conventional interventions.

The availability of landward accommodation space is particularly relevant. Beaches backed by preserved dunes or areas with limited urban development may have more space to adjust. In contrast, rigid infrastructure can restrict landward migration and reduce adaptation space [58].

F_A and F_W are not intended to replace hydrodynamic modelling or inundation analysis. Rather, they translate physical inundation outputs into normalized measures of the dry beach space that remains available. Using F_A and F_W together allows beaches of different sizes to be compared. It also shows whether residual surface area and mean width evolve in a broadly similar way. This simple interpretation may help coastal managers compare model results. It can also identify sites where the remaining beach space becomes particularly limited or spatially unbalanced.

4.4. Limitations and Scope of the Indicators

Several limitations should be considered when interpreting these results. First, the scenarios retain the present-day beach morphology and do not explicitly account for sediment redistribution, shoreline retreat, or other morphodynamic adjustments [59]. F_A and F_W represent the residual dry beach space under the imposed inundation levels and present-day morphology. They should not be interpreted as predictions of future equilibrium beach morphology.

Second, potential future changes in wave climate are not explicitly considered. Changes in storm intensity and trajectories may modify offshore wave conditions and consequently the associated wave run-up [60,61]. The calculated values should therefore be interpreted within the forcing assumptions adopted in the underlying inundation analysis.

Finally, F_A and F_W describe only the physical availability of dry beach surface area and mean width. They do not directly account for environmental quality, recreational intensity, economic value, ecological functions, or minimum spatial requirements for specific beach uses. Accordingly, residual functionality is used here only in a spatial sense. It describes the amount and configuration of dry beach space remaining relative to the reference condition. F_A and F_W should therefore be interpreted as indicators of residual spatial functionality, rather than as a comprehensive assessment of overall beach functionality.

5. Conclusions

The analysis shows that sea-level rise may lead to markedly different reductions in dry beach surface area and width even among geographically close beaches. These differences are controlled not only by the climate scenario considered but also by local beach morphology and configuration.

The F_A and F_W indicators provide a simple means of expressing the proportion of dry beach surface area and mean width remaining relative to the reference condition. Their main advantage is that they allow direct comparison among beaches of different sizes and morphologies. They also allow surface-area and width responses to be interpreted together.

The five beaches exhibit clearly contrasting responses. Torreguadiaro consistently retains the highest residual functionality, whereas Rinconcillo undergoes a pronounced reduction toward the end of the century. Under the 2081–2100 RCP 8.5 scenario, Torreguadiaro retains 75.6% of its reference surface area and 65.3% of its reference mean width. Rinconcillo retains only 7.1% and 17.6%, respectively. Los Toruños represents the most unfavorable case under the conditions considered. Residual surface area and width do not always evolve in parallel. This divergence is marked at Rinconcillo, whereas both indicators remain relatively close at Malagueta.

The residual-functionality analysis uses inundation levels that include wave run-up. As a result, substantial reductions in dry beach space are already evident under present-day conditions. In the present study, wave run-up is therefore treated as part of the underlying physical forcing rather than as a newly assessed process, providing the basis for evaluating the dry surface area and width that remain available under each scenario.

From a coastal management perspective, the results indicate that uniform adaptation responses should not be applied across different beaches. Local morphology, the amount of space remaining available, and the potential to maintain or recover beach width should be considered when assessing adaptation alternatives.

F_A and F_W are not intended to represent all dimensions of beach functionality. Rather, they provide complementary indicators of residual spatial functionality, translating physical inundation results into normalized measures of the dry beach space that remains available. Their joint interpretation adds information on whether residual surface area and mean width evolve proportionally, while retaining a form that is readily interpretable and comparable for coastal management purposes.

Author Contributions: Conceptualization, A.C.-d.-V., J.J.M.-P. and J.M.V.-P.; methodology, A.C.-d.-V., J.J.M.-P. and F.C.-d.-V.; formal analysis, A.C.-d.-V., J.J.M.-P. and J.M.V.-P.; data curation, A.C.-d.-V., C.P.-M. and P.L.-G.; writing—original draft preparation, A.C.-d.-V. and J.J.M.-P.; writing—review and editing, A.C.-d.-V., F.C.-d.-V., J.M.V.-P., C.P.-M., J.J.A.d.R., P.L.-G., B.J.-A. and J.J.M.-P.; visualization, A.C.-d.-V. and J.J.M.-P.; supervision, A.C.-d.-V., J.M.V.-P. and J.J.M.-P.; project administration, J.J.M.-P. and J.M.V.-P.; funding acquisition, J.J.M.-P. and J.M.V.-P. All authors have read and agreed to the published version of the manuscript.

Funding: This research was funded by Project PCM_00124 through the European Union's Next Generation EU funds under the Recovery, Transformation and Resilience Plan, co-financed by the Regional Ministry of University, Research and Innovation of the Andalusian Regional Government (Junta de Andalucía), Spain.

Institutional Review Board Statement: Not applicable.

Informed Consent Statement: Not applicable.

Data Availability Statement: The data used in this study were derived from results previously reported by Contreras-de-Villar et al. [35] and are summarized in the present article. Further inquiries can be directed to the corresponding author.

Conflicts of Interest: The authors declare no conflicts of interest.

References

1. Gilman, E.L.; Ellison, J.; Duke, N.C.; Field, C. Threats to mangroves from climate change and adaptation options: A review. *Aquat. Bot.* **2008**, *89*, 237–250. [CrossRef]
2. Thuiller, W.; Lavorel, S.; Araújo, M.B.; Sykes, M.T.; Prentice, I.C. Climate change threats to plant diversity in Europe. *Proc. Natl. Acad. Sci. USA* **2005**, *102*, 8245–8250. [CrossRef] [PubMed]
3. Sheffield, P.E.; Landrigan, P.J. Global climate change and children's health: Threats and strategies for prevention. *Environ. Health Perspect.* **2011**, *119*, 291–298. [CrossRef] [PubMed]
4. Nhemachena, C.; Nhamo, L.; Matchaya, G.; Nhemachena, C.R.; Muchara, B.; Karuaihe, S.T.; Mpandeli, S. Climate change impacts on water and agriculture sectors in Southern Africa: Threats and opportunities for sustainable development. *Water* **2020**, *12*, 2673. [CrossRef]
5. Hrabok, M.; Delorme, A.; Agyapong, V.I.O. Threats to mental health and well-being associated with climate change. *J. Anxiety Disord.* **2020**, *76*, 102295. [CrossRef] [PubMed]
6. Holgate, S.J.; Woodworth, P.L. Evidence for enhanced coastal sea level rise during the 1990s. *Geophys. Res. Lett.* **2004**, *31*, L07305. [CrossRef]
7. IPCC. *Climate Change 2013: The Physical Science Basis*; Cambridge University Press: Cambridge, UK, 2013.
8. IPCC. *Climate Change 2022: Impacts, Adaptation and Vulnerability*; Cambridge University Press: Cambridge, UK, 2022.
9. Vousdoukas, M.I.; Ranasinghe, R.; Mentaschi, L.; Plomaritis, T.A.; Athanasiou, P.; Luijendijk, A.; Feyen, L. Sandy coastlines under threat of erosion. *Nat. Clim. Change* **2020**, *10*, 260–263. [CrossRef]
10. Aguilera-Vidal, M.; Muñoz-Perez, J.J.; Contreras, A.; Contreras, F.; Lopez-Garcia, P.; Jigena, B. Increase in the erosion rate due to the impact of climate change on sea level rise: Victoria Beach, a case study. *J. Mar. Sci. Eng.* **2022**, *10*, 1912. [CrossRef]
11. Balica, S.F.; Wright, N.G.; van der Meulen, F. A flood vulnerability index for coastal cities and its use in assessing climate change impacts. *Nat. Hazards* **2012**, *64*, 73–105. [CrossRef]
12. Ezer, T. A demonstration of a simple methodology of flood prediction for a coastal city under threat of sea level rise: The case of Norfolk, VA, USA. *Earth's Future* **2022**, *10*, e2022EF002786. [CrossRef]
13. Vousdoukas, M.I.; Mentaschi, L.; Voukouvalas, E.; Verlaan, M.; Feyen, L. Extreme sea levels on the rise along Europe's coasts. *Earth's Future* **2017**, *5*, 304–323. [CrossRef]
14. Viigand, K.; Eelsalu, M.; Soomere, T. Inherent non-stationarity in the GEV distribution for extreme sea levels: Implications for coastal vulnerability in the Baltic Sea. *Ocean Eng.* **2025**, *341*, 122681. [CrossRef]
15. Hung, N.T.; Cuong, V.D.; Thanh, N.T.; Quan, T.Q. Simulation of coastal flooding under extreme weather patterns for Quang Tri Province, Vietnam. *Estuaries Coasts* **2026**, *49*, 22. [CrossRef]
16. Toubes, D.R.; Gössling, S.; Hall, C.M.; Scott, D. Vulnerability of coastal beach tourism to flooding: A case study of Galicia, Spain. *Environments* **2017**, *4*, 83. [CrossRef]
17. Houston, J.R. The value of Florida beaches. *Shore Beach* **2013**, *81*, 4–11.

18. Toimil, A.; Losada, I.J.; Álvarez-Cuesta, M.; Le Cozannet, G. Demonstrating the value of beaches for adaptation to future coastal flood risk. *Nat. Commun.* **2023**, *14*, 3474. [CrossRef] [PubMed]
19. Calvillo García, Y.; Ramírez-Herrera, M.T.; Delgado-Trejo, C.; Legorreta-Paulin, G.; Corona, N. Modeling sea-level change, inundation scenarios, and their effect on the Colola Beach Reserve—A nesting-habitat of the black sea turtle, Michoacán, Mexico. *Geofís. Int.* **2015**, *54*, 179–190. [CrossRef]
20. Grases, A.; Gracia, V.; García-León, M.; Lin-Ye, J.; Sierra, J.P. Coastal flooding and erosion under a changing climate: Implications at a low-lying coast (Ebro Delta). *Water* **2020**, *12*, 346. [CrossRef]
21. Agulles, M.; Jordà, G.; Lionello, P. Flooding of sandy beaches in a changing climate: The case of the Balearic Islands (NW Mediterranean). *Front. Mar. Sci.* **2021**, *8*, 760725. [CrossRef]
22. Sánchez-Artús, X.; Gracia, V.; Espino, M.; Sierra, J.P.; Pinyol, J.; Sánchez-Arcilla, A. Present and future flooding and erosion along the NW Spanish Mediterranean coast. *Front. Mar. Sci.* **2023**, *10*, 1125138. [CrossRef]
23. Bozzeda, F.; Ortega, L.; Costa, L.L.; Fanini, L.; Barboza, C.A.M.; McLachlan, A.; Defeo, O. Global patterns in sandy beach erosion: Unraveling the roles of anthropogenic, climatic and morphodynamic factors. *Front. Mar. Sci.* **2023**, *10*, 1270490. [CrossRef]
24. Janda, C.N.; Warrick, J.A.; Buscombe, D.; Batiste, S. Shoreline change of Western Long Island, New York, from satellite-derived shorelines. *Coasts* **2025**, *5*, 2. [CrossRef]
25. Muñoz-Pérez, J.J.; Payo, A.; Roman-Sierra, J.; Navarro, M.; Moreno, L. Optimization of beach profile spacing: An applicable tool for coastal monitoring. *Sci. Mar.* **2012**, *76*, 791–798. [CrossRef]
26. Contreras, A.; Muñoz-Perez, J.J.; Contreras, F.; Gomez-Pina, G.; Ruiz-Ortiz, V.; Chamorro, G.; Cabrera, P. A design parameter for reef beach profiles—A methodology applied to Cadiz, Spain. *J. Mar. Sci. Eng.* **2020**, *8*, 323. [CrossRef]
27. Contreras-de-Villar, A.; Gómez-Pina, G.; Muñoz-Pérez, J.J.; Contreras-de-Villar, F.; López-García, P.; Ruiz-Ortiz, V. New design parameters for biparabolic beach profiles (SW Cadiz, Spain). *Rev. Constr.* **2019**, *18*, 432–444. [CrossRef]
28. Contreras-de-Villar, F.; García, F.J.; Muñoz-Perez, J.J.; Contreras-de-Villar, A.; Ruiz-Ortiz, V.; López-García, P.; Jigena-Antelo, B. Analysis of topographic surveys with RPAS in steep coastal dunes. *Land* **2023**, *12*, 1729. [CrossRef]
29. Lopez-Garcia, P.; Muñoz-Perez, J.J.; Contreras, A.; Vidal, J.; Jigena, B.; Santos, J.J.; Romero, J.; Contreras, F. Error on the estimation of sand size parameters when using small diameter sieves and a solution. *Front. Mar. Sci.* **2021**, *8*, 738479. [CrossRef]
30. Santos-Vendoiro, J.J.; Muñoz-Perez, J.J.; Lopez-García, P.; Jodar, J.M.; Mera, J.; Contreras, A.; Contreras, F.; Jigena, B. Evolution of sediment parameters after a beach nourishment. *Land* **2021**, *10*, 914. [CrossRef]
31. Fontán-Bouzas, Á.; Andriolo, U.; Silva, P.A.; Baptista, P. Wave impact analysis on a beach-dune system to support coastal management and nourishment works: The showcase of Mira, Portugal. *Front. Mar. Sci.* **2022**, *9*, 861569. [CrossRef]
32. Pranzini, E.; Cinelli, I.; Anfuso, G. Beaches' expulsion from paradise: From a natural to an artificial littoral in Tuscany (Italy). *Coasts* **2024**, *4*, 697–725. [CrossRef]
33. Muñoz-Pérez, J.J.; Gutierrez-Mas, J.M.; Parrado, J.M.; Moreno, L. Sediment transport velocity by tracer experiment at Regla Beach (Spain). *J. Waterw. Port Coast. Ocean Eng.* **1999**, *125*, 332–335. [CrossRef]
34. Gobierno de España, Ministerio de Agricultura, Alimentación y Medio Ambiente. *Elaboración de los Mapas de Peligrosidad y Riesgo Requeridos por RD 903/2010 en la Costa Española*; Gobierno de España, Ministerio de Agricultura, Alimentación y Medio Ambiente: Madrid, Spain, 2010.
35. Contreras-de-Villar, A.; Muñoz-Perez, J.J.; Contreras-de-Villar, F.; Vidal-Perez, J.M.; Perez-Moreno, C.; Alonso del Rosario, J.J.; Lopez-Garcia, P.; Jigena-Antelo, B. Future sea level rise impacts on sandy beaches under contrasting tidal regimes: The role of wave run-up in southern Spain. *Water* **2026**, *18*, 1407. [CrossRef]
36. Agencia Estatal de Meteorología (AEMET). *Guía de Escenarios Regionalizados de Cambio Climático Sobre España a Partir de los Resultados del IPCC-AR5*; Agencia Estatal de Meteorología (AEMET): Madrid, Spain, 2017.
37. Instituto de Hidráulica Ambiental de Cantabria. *Visor C3E*; Instituto de Hidráulica Ambiental de Cantabria: Santander, Spain, 2016.
38. Puertos del Estado. *PORTUS: Información Oceanográfica y Meteorológica*; Puertos del Estado: Madrid, Spain, 2022.
39. Puertos del Estado. *REDMAR: Red de Mareógrafos de Puertos del Estado*; Puertos del Estado: Madrid, Spain, 2023.
40. Ministerio para la Transición Ecológica. *Guía para el Acceso a los Datos de Proyecciones Climáticas Regionales Marinas en España*; Ministerio para la Transición Ecológica: Madrid, Spain, 2016.
41. UTE Ecoatlántico. *Estudio Ecocartográfico del Litoral de la Provincia de Cádiz. Estudio de Mareas*; UTE Ecoatlántico: Cádiz, Spain, 2013.
42. UTE INTECSA-INARSA. *Ecocartografía del Litoral de la Provincia de Málaga*; UTE INTECSA-INARSA: Madrid, Spain, 2004.
43. Jigena-Antelo, B.; Estrada-Ludeña, C.; Howden, S.; Rey, W.; Paz-Acosta, J.; Lopez-García, P.; Salazar-Rodriguez, E.; Endrina, N.; Muñoz-Pérez, J.J. Evidence of sea level rise at the Peruvian coast (1942–2019). *Sci. Total Environ.* **2023**, *859*, 160082. [CrossRef] [PubMed]
44. Losada, I.J.; Lara, J.L.; Guanche, R.; Gonzalez-Ondina, J. Numerical analysis of wave overtopping of rubble mound breakwaters. *Coast. Eng.* **2008**, *55*, 47–62. [CrossRef]
45. Lara, J.L.; Losada, I.J.; Maza, M.; Guanche, R. Breaking solitary wave evolution over a porous underwater step. *Coast. Eng.* **2011**, *58*, 837–850. [CrossRef]

46. Stockdon, H.F.; Holman, R.A.; Howd, P.A.; Sallenger, A.H. Empirical parameterization of setup, swash, and runup. *Coast. Eng.* **2006**, *53*, 573–588. [CrossRef]
47. Brunel, C.; Sabatier, F. Pocket beach vulnerability to sea-level rise. *J. Coast. Res.* **2007**, *50*, 604–609. [CrossRef]
48. Bon de Sousa, L.; Loureiro, C.; Ferreira, O. Morphological and economic impacts of rising sea levels on cliff-backed platform beaches in southern Portugal. *Appl. Geogr.* **2018**, *99*, 31–43. [CrossRef]
49. Thieblemont, R.; Le Cozannet, G.; Rohmer, J.; Toimil, A.; Álvarez-Cuesta, M.; Losada, I.J. Deep uncertainties in shoreline change projections: An extra-probabilistic approach applied to sandy beaches. *Nat. Hazards Earth Syst. Sci.* **2021**, *21*, 2257–2276. [CrossRef]
50. Castelle, B.; Ritz, A.; Marieu, V.; Nicolae Lerma, A.; Vandenhove, M. Primary drivers of multidecadal spatial and temporal patterns of shoreline change derived from optical satellite imagery. *Geomorphology* **2022**, *413*, 108360. [CrossRef]
51. Masselink, G.; Brooks, S.; Poate, T.; Stokes, C.; Scott, T. Coastal dune dynamics in embayed settings with sea-level rise—Examples from the exposed and macrotidal north coast of SW England. *Mar. Geol.* **2022**, *450*, 106853. [CrossRef]
52. Alonso del Rosario, J.J.; Yin, D.; Vidal Pérez, J.M.; Coronil Huertas, D.J.; Blázquez Gómez, E.; Pavón Quintana, S.; Muñoz Pérez, J.J.; Torrecillas, C. The extremal value analysis of sea level in the Gulf of Cádiz and Alborán Sea: A new methodology and the resilience of critical infrastructures. *J. Mar. Sci. Eng.* **2025**, *13*, 1567. [CrossRef]
53. Klein, R.J.T.; Nicholls, R.J. Assessment of coastal vulnerability to climate change. *Ambio* **1999**, *28*, 182–187.
54. Ministerio para la Transición Ecológica y el Reto Demográfico. *Plan Nacional de Adaptación al Cambio Climático 2021–2030*; Gobierno de España: Madrid, Spain, 2020.
55. Bongarts Lebbe, T.; Rey-Valette, H.; Chaumillon, É.; Camus, G.; Almar, R.; Cazenave, A.; Claudet, J.; Rocle, N.; Meur-Férec, C.; Viard, F.; et al. Designing coastal adaptation strategies to tackle sea level rise. *Front. Mar. Sci.* **2021**, *8*, 740602. [CrossRef]
56. Setter, R.O.; Han, R.X.; Tavares, K.-D.; Newfield, C.; Terry, A.; Roberson, I.M.; Tarui, N.; Coffman, M. Managing retreat for sandy beach areas under sea level rise. *Sci. Rep.* **2023**, *13*, 11920. [CrossRef] [PubMed]
57. Hernández-Delgado, E.A. Coastal restoration challenges and strategies for Small Island Developing States in the face of sea level rise and climate change. *Coasts* **2024**, *4*, 235–286. [CrossRef]
58. Lansu, E.M.; Reijers, V.C.; Höfer, S.; Luijendijk, A.; Rietkerk, M.; Wassen, M.J.; Lammerts, E.J.; van der Heide, T. A global analysis of how human infrastructure squeezes sandy coasts. *Nat. Commun.* **2024**, *15*, 432. [CrossRef] [PubMed]
59. Ranasinghe, R.; Callaghan, D.P.; Li, F.; Wainwright, D.J.; Duong, T.M. Assessing coastline recession for adaptation planning: Sea level rise versus storm erosion. *Sci. Rep.* **2023**, *13*, 8286. [CrossRef] [PubMed]
60. Grabemann, I.; Weisse, R. Climate change impact on extreme wave conditions in the North Sea: An ensemble study. *Ocean Dyn.* **2008**, *58*, 199–212. [CrossRef]
61. Wolf, J.; Woolf, D.; Bricheno, L. Impacts of climate change on storms and waves relevant to the coastal and marine environment around the UK. *MCCIP Sci. Rev.* **2020**, *2020*, 132–157.

Disclaimer/Publisher's Note: The statements, opinions and data contained in all publications are solely those of the individual author(s) and contributor(s) and not of MDPI and/or the editor(s). MDPI and/or the editor(s) disclaim responsibility for any injury to people or property resulting from any ideas, methods, instructions or products referred to in the content.